PERGAMON

Vision Research 39 (1999) 2841–2852

Vision Research

A wide-angle gradient index optical model of the crystalline lens and eye of the octopus

W.S. Jagger [a,*], P.J. Sands [b]

[a] *Department of Biological Sciences, Monash University, Clayton, Victoria 3168, Australia*
[b] *CSIRO Division of Forestry and Forest Products, GPO Box 252-12, Hobart, Tasmania 7001, Australia*

Received 9 June 1997; received in revised form 27 July 1998

Abstract

Cephalopods and fish have had no common ancestor since the Cambrian, and their eyes are a classic example of convergent evolution. The octopus has no cornea, and immerson renders the trout cornea optically ineffective. As a result, the nearly spherical lens is responsible for all refraction in these eyes. In spite of the fact that the octopus lens consists of two joined parts, while the trout lens consists of one part, we show here that their optical properties are very similar. An index gradient bends rays within these lenses, adding power and correcting spherical aberration. High spherical symmetry in both lenses strongly reduces other monochromatic aberrations and yields a wide field of vision, advantageous in attack and evasion. The octopus Mattheissen's ratio, 2.83, an inverse measure of light-gathering power, lies above the trout value of 2.38 but within the range of values reported for fish. Strong uncorrected longitudinal chromatic aberration is nearly identical in both animals as a result of similar lens protein optical properties, and will limit resolution. We discuss how animal lifestyle requirements and lens material properties influence the design of these eyes.

Keywords: Octopus; Trout; Optics; Eye; Lens; Convergent evolution

1. Introduction

Cephalopods and fish have independently evolved superficially similar eyes (Darwin, 1872; Packard, 1972). The eyes of two visual predators, octopus and trout, have nearly spherical lenses which perform the entire task of image formation. Does the superficial resemblance between these eyes signal an underlying fundamental similarity? We examined the structure and optical function of the octopus eye and lens for comparison with those of the trout, treated here earlier (Jagger, 1992; Jagger & Muntz, 1993; Jagger, 1996; Jagger & Sands, 1996; Jagger, 1997).

The optics of the octopus eye have been studied for over a century. Beer (1897) and Hess (1909) measured accommodation by lens movement of up to 14 D in octopus induced by drugs and electrical stimulation. Heidermanns (1928) described the field of view of octopus, and observed chromatic fringes in the images formed by an octopus lens, demonstrating that the lens is not chromatically corrected. Sroczyński and Muntz (1985) found that the focal length varied by about 4% over the wavelength range 450–700 nm due to longitudinal chromatic aberration and that Mattheissen's ratio (focal length divided by lens radius) was about 2.7. The same authors (Sroczyński & Muntz, 1987) reported strong paraxial astigmatism in the octopus *Eledone cirrhosa*. Significant longitudinal spherical aberration was reported for an octopus lens (Sivak, 1991).

The anatomy, physiology, and development of the cephalopod eye have also been the subject of study. Neuroanatomy of the octopus visual system was described by Young (1971), and development of the cephalopod eye and optic lobe was studied by Arnold (1967) and Wentworth and Muntz (1992). West, Sivak, Pasternak and Piatigorsky (1994) followed the development of crystallins in the squid lens, and cephalopod pupillary response to light was described by Muntz (1977).

The visual capabilities of *Octopus australis* and *O. pallidus* (species which differ little) were measured using

* Corresponding author.
E-mail address: wsjagger@vaxc.ccmonash.edu.au (W.S. Jagger)

0042-6989/99/$ - see front matter
PII: S0042-6989(99)00012-7

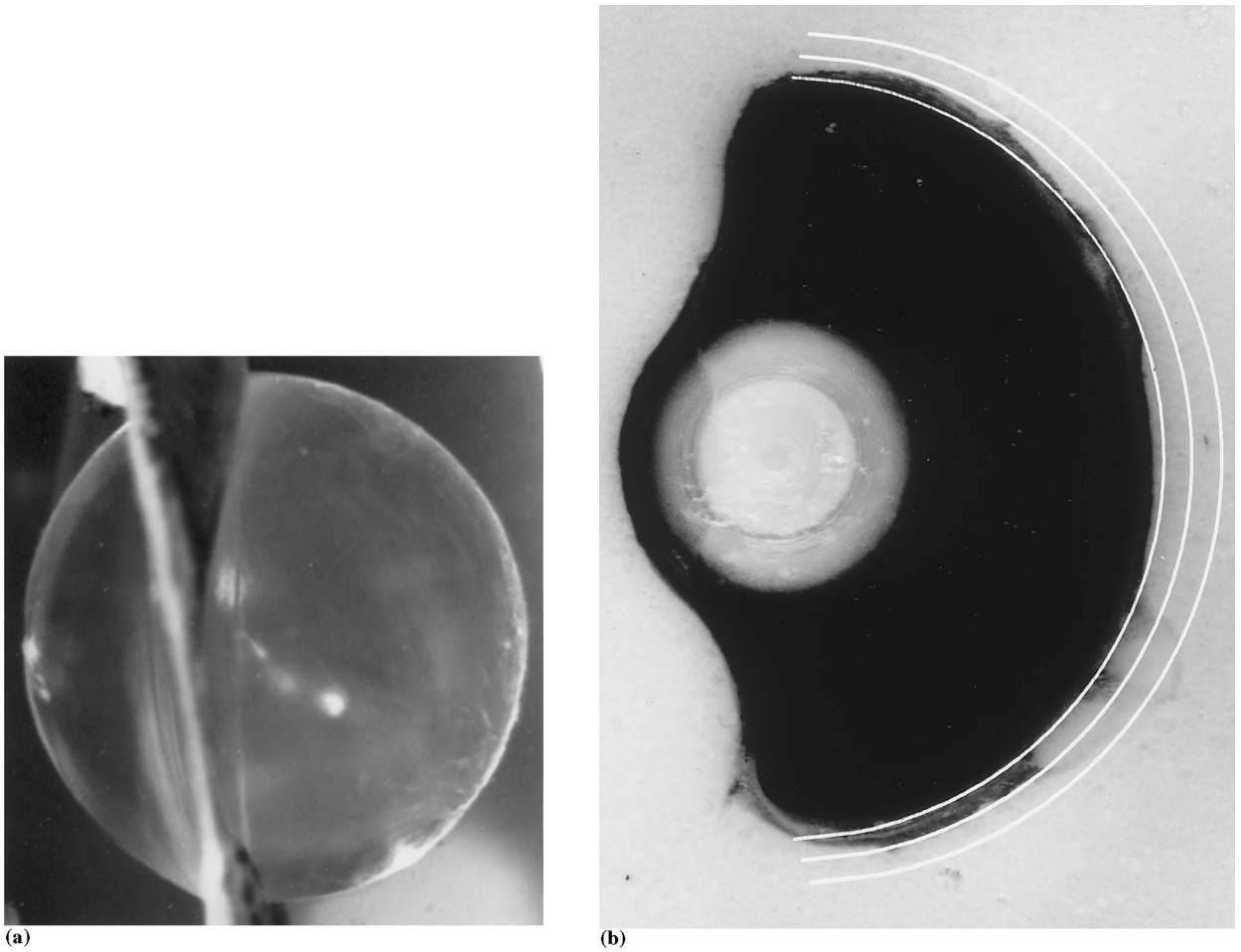

Fig. 1. (a) Photograph of an octopus lens from the side, with anterior pole to the left. Part of the suspending opaque collar remains attached. Axial length 6.17 mm. (b) Horizontal frozen section of a freshly excised octopus eye maintained under pressure during freezing to maintain its form, of lens axial thickness 3.54 mm. Its pupil is closed. Curves are three model focal surfaces for objects at infinity (closest to lens), and 100 and 50 mm distant. In this figure, down is towards the arms and up is towards the mantle.

behavioural methods by Muntz and Gwyther (1988, 1989), who found that the grating discrimination limit lay between 3 and 7 c/deg. Optokinetic responses in small octopus occur for spatial frequencies below 0.5 c/deg (Packard, 1969). Octopus are able to discriminate polarized light (Moody & Parriss, 1960).

2. Methods

Definitions, conventions, abbreviations and methods employed are given by Jagger and Sands (1996). Variations specific to the octopus are described below.

2.1. The octopus eye

Specimens of *O. australis* and *O. pallidus* were trapped near Queenscliff, Victoria, and kept in tanks for no longer than 3 weeks. Animals were killed and eyes excised immediately before measurements. The osmolarity of the octopus posterior chamber is about 10% higher than sea water (Amoore, Rodgers & Young, 1959). Calculations show that the increase in refractive index over that of sea water induced by this increase is optically negligible; isolated lenses were therefore held in sea water at room temperature (18–20°C) during measurements. No changes in lens dimensions ($>0.5\%$) or clarity were noted after more than 2 h in sea water. As it was difficult to obtain wild specimens of uniform size, lenses studied were of axial thickness ranging from 3.2 to 6.3 mm, from animals ranging in weight from 90 to 350 g. No significant differences other than size were noted within this group. Along the eye's axis, the terms anterior (towards the object) and posterior (towards the retina) are employed, as for vertebrate eyes.

3. Results

3.1. Optical anatomy

Fig. 1a shows an octopus lens seen from the side, perpendicular to the optical axis, and Fig. 1b a horizontal section of an octopus eye. Octopus lenses are nearly spherical, with average axial thickness 5% smaller than the equatorial diameter, and consist of axially symmetric anterior and posterior parts. Fig. 2 shows the basic structure of an octopus eye. The lens is supported in the eye by a dark flexible opaque collar, consisting of a suspensory ligament and lentigenic cells. This collar extends a small distance inside the lens at the junction of the anterior and posterior parts, where it acts as a circular aperture stop. The iris lies on this collar and the lens anterior surface, forming a pupil ranging from round (at nearly full lens aperture) to a progressively narrower horizontal slit. Lens external shape is described in Table 1. The octopus eye is not rigid but depends upon internal pressure to maintain its shape.

The internal refractive structure of a typical lens measured with the Pulfrich areal refractometer is shown in Fig. 3a. This somewhat irregular structure shows considerable variation from one lens to another. The isoindicial curves of the anterior lens portion join smoothly with those of the posterior section, and are generally concentric with the lens surfaces. Gradients measured perpendicular to the axis are shown in Fig. 3b.

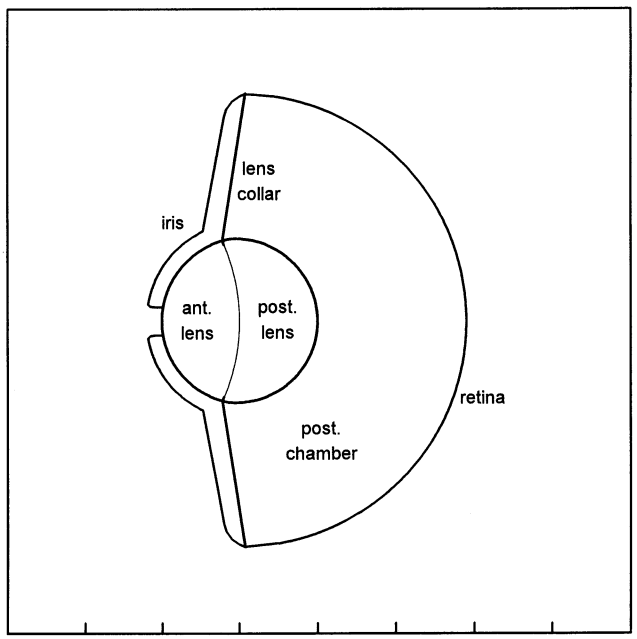

Fig. 2. Schematic vertical section through an octopus eye. Model scale units (2 units = lens axial thickness) are marked on the lower border.

Table 1
Lens measurements ($n = 13$ for external and $n = 5$ for internal structure) and model parameters[a]

	Normalized measurement	Normalized model
External structure		
Axial thickness	Tax = 2.000	Tax = 2.000
Equatorial radius	Req = 1.048 ± 0.02 S.D.	Req = 1.048
Anterior surface shape	$A_x = 1.051 \pm 0.165$ S.D.	$R_0 = 1.060$
	$A_y = 1.069 \pm 0.055$ S.D.	
Ant.-post. Junction surface		$R_0 = -2.47$
Posterior surface shape	$A_x = 1.041 \pm 0.045$ S.D.	$R_0 = -1.045$
	$A_y = 1.050 \pm 0.033$ S.D.	
Collar distance from ant. pole	0.77 ± 0.04 S.D.	0.77
External medium index (550 nm)	1.3410 (sea water)	1.3410
Internal refractive structure		
Core index (550 nm)	1.509 ± 0.01 S.D.	1.502
Cortex index (550 nm)	1.357 ± 0.01 S.D.	1.363
Gradient polynomial coefficients		
Degree 2		0.73
Degree 6		0.16
Degree 8		−0.05
Degree 10		0.16

[a] Normalization, by setting lens axial thickness equal to 2.000, allows calculation and comparison of average shapes etc. from measurements on eyes of differing sizes. A_x and A_y are measured surface semi-axes, with A_x measured along the optical axis

3.2. Optical properties of the lens

Fig. 4 shows a meridional fan of parallel laser beams traversing the lens in the simplified Hartmann test with incident beams parallel to the axis (a) and inclined at 45° (b). The focal length is 2.90 (± 0.06 S.D.) times the axial radius. The lens scatters light, as is evident from the visibility from the side of laser beams traversing the lens, with internal concentric zones scattering more strongly. Schlieren photographs of the lens back aperture (Fig. 5) show that, as opposed to the trout lens, zonal aberration is minimal, aberration correction is generally uniform over the lens, and radially oriented structure is absent. Filamentous structures about 30 μm thick that may be expected to scatter light appear in a nearly random pattern over the aperture.

Fig. 6 shows plots of longitudinal spherical aberration measured from the course of refracted laser beams in the Hartmann test on five octopus lenses. There is generally good correction for this aberration on axis (a) and at 45° to the axis (b). However, strong longitudinal chromatic aberration causes a chromatic shift in focus of about 4% over the spectral range of 450–700 nm (Fig. 7a).

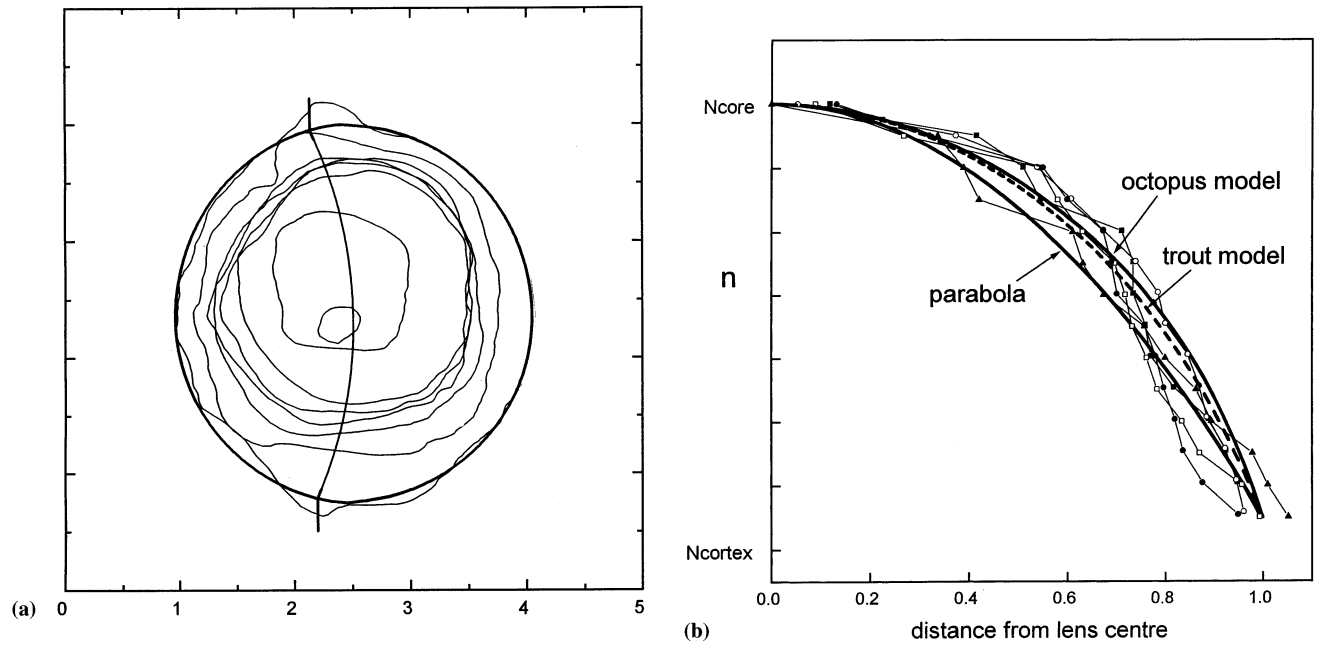

Fig. 3. (a) The distribution of refractive index within an octopus lens. Internal isoindicial curves of an octopus lens in the plane of the axis, anterior to the left. Contour interval 0.02 index units, from 1.38 to 1.52. Lens outline and the boundary between anterior and posterior parts are also shown. Scale in mm. (b) Measured gradient curves from five lenses measured in the equatorial plane, normalized to similar values of core and cortical index to facilitate shape comparison. A parabolic curve is shown, as well as the gradient curves used for the model lenses of the octopus and trout (from Jagger & Sands, 1996). Core and cortical indices for the octopus model are 1.502 and 1.363, respectively, and for the trout model 1.538 and 1.372, respectively.

3.3. Construction of the basic lens model

A computer model (Table 1, Fig. 8) of the octopus lens was constructed from anatomical measurements for use with the ray-tracing program Drishti (Sands, 1984; Jagger & Sands, 1996). The measured anterior and posterior lens surfaces differ insignificantly from spheres. These surfaces, assumed spherical in the model, have different radii and are not concentric. The junction surface within the lens between anterior and posterior parts was taken as spherical, joining the lens centre and the collar intersection point at the surface. The internal isoindicial curves were taken as concentric with the external surfaces. The model internal index gradient (core and cortical indices and gradient form) was then adjusted within the measured ranges by successive approximation to yield the observed focal length and longitudinal spherical aberration of the lens. The narrow constraints on parameters and required model behaviour make it highly unlikely that a significantly different solution exists. The shape of the model internal index gradient (Fig. 3b) is given by a tenth degree polynomial:

$$n(r) = n_{\text{core}}(1 + 0.73{\cdot}K{\cdot}r^2 + 0.16{\cdot}K{\cdot}r^6 - 0.05{\cdot}K{\cdot}r^8 = 0.16{\cdot}K{\cdot}r^{10})$$

where $K = (n_{\text{cortex}}/n_{\text{core}}) - 1$. A change in the least significant figure of one of these polynomial coefficients results in a significant deterioration in aberration correction. At different wavelengths, the index of the medium, cortex and core change because of chromatic dispersion (Fig. 7b), although the gradient shape remains unchanged. Dispersion of the medium is that of sea water (Houstoun, 1930; Vine, 1972). Model dispersion curves describing lens material are similar to and based upon those of the trout model (Jagger & Sands, 1996). Scattering structures can be included implicitly into the lens model as small perturbations.

3.4. Model lens and eye behaviour

A meridional ray fan traced through the model shown in Fig. 8a forms a sharp point image both on axis (Fig. 8b) and 45° off axis (Fig. 8c). The model axial focal length is 2.90 times the lens axial radius, equal to that observed, and the retina in a frozen section coincides with the image surface (Figs. 1b and 8b). The calculated longitudinal spherical aberration for this model is shown as a solid line superimposed on the measured points of Fig. 6, and is in good agreement with these measurements. Calculated model chromatic aberration coincides with the curve describing the measurements in Fig. 7a. Fig. 9 shows the calculated monochromatic pointspread function (PSF) and modulation transfer function (MTF) of the model lens. These model curves represent upper limits to resolution expected from an octopus lens. Resolution of a real lens may be degraded from these values by structural irregu-

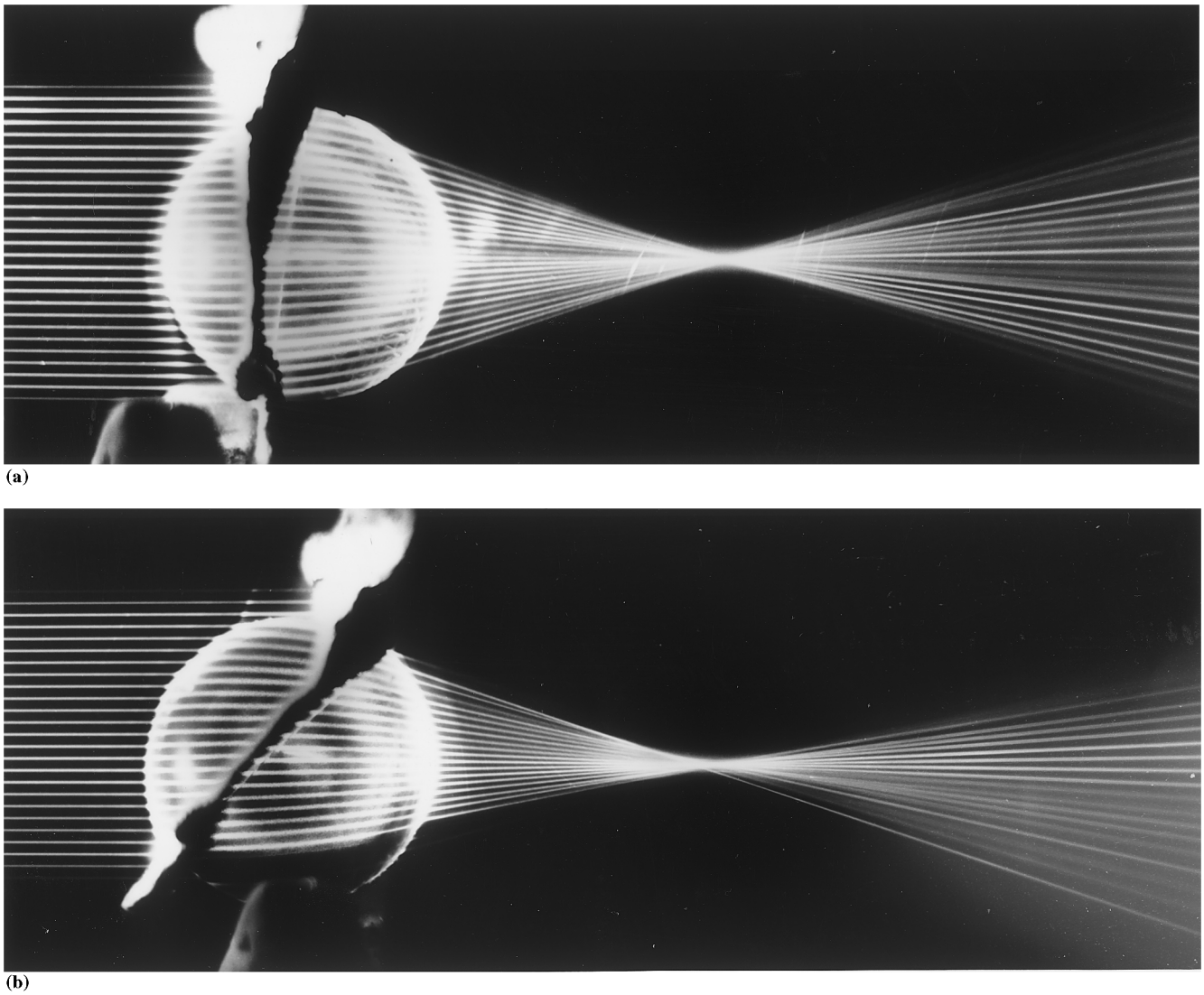

Fig. 4. Meridional fan of parallel laser beams refracted by an octopus lens, showing lens focal length, course of beams within the lens, aberration correction, and retinal irradiance decrease with peripheral angle. Beam spacing is 0.25 mm. (a) Beams parallel to the axis; and (b) beams inclined at 45° to the axis. Fewer beams are transmitted in (b) than in (a) because the full pupil is foreshortened, resulting in a lower retinal irradiance. Glare obscures the sharp focus achieved for both field angles.

larity and other factors. Calculated model retinal irradiance (Fig. 10) is shown for a full pupil, and for horizontal slit pupils of 0.5 and 0.17 width.

4. Discussion

The eyes of octopus and trout (Jagger & Sands, 1996) (Fig. 11) present a classic example of convergent evolution. We can now compare optical structure and function of these visual predators in detail.

4.1. The optically ineffective fish cornea and the lack of a cornea in octopus

In both octopus and trout, the lens assumes the entire task of image formation. In land species, the cornea usually supplies substantial optical power, and its shape is axially symmetric to fulfil this role. But the fish cornea has negligible optical power because it is immersed in fluid of similar index, and its exact shape is therefore optically irrelevant. The trout cornea is axially asymmetric and apparently serves as a streamlined window, protecting the weakly suspended lens from fluid forces while swimming (Jagger & Sands, 1996). The octopus lens, with no cornea to protect it, is more firmly held around its periphery by its suspending collar.

4.2. Lens structure and spherical symmetry

Octopus and fish lenses both display a high degree of spherical symmetry. The axial thickness of the octopus lens is 5% less than its equatorial diameter, while the

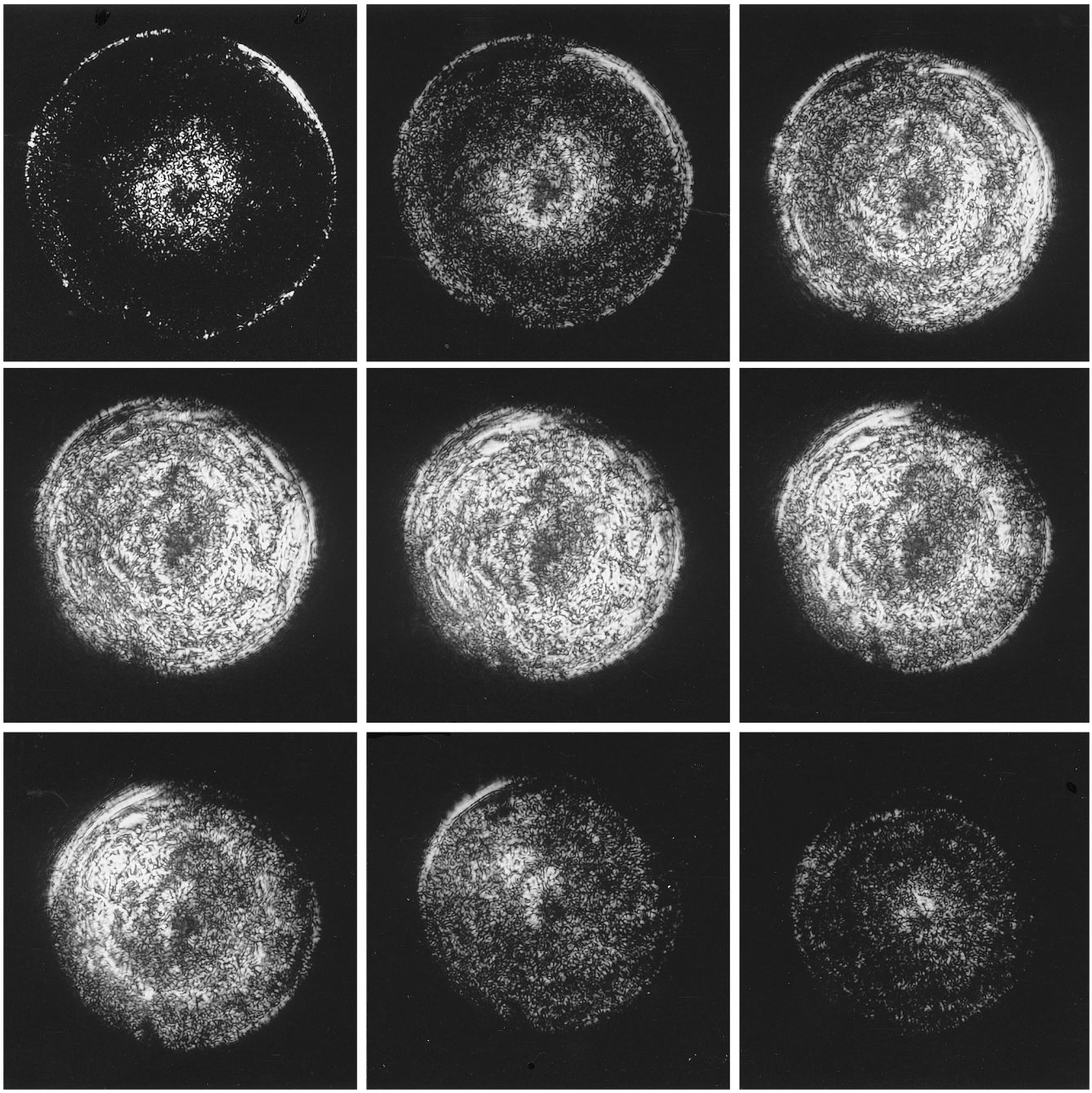

Fig. 5. Schlieren photographs of the back aperture of an octopus lens. Overall uniformity of illumination indicates good aberration correction. From the upper left to the lower right, proceeding left to right, the spacing in μm relative to best focus is, with negative numbers denoting outside focus: −900, −500, −200, −100, 0, +100, +200, +500. +900.

trout lens is more spherical, with a corresponding value of 2% (Jagger & Sands, 1996). This symmetry allows relatively uniform image quality over a wide field. While the fish lens is composed of concentric shells of lens fibres generated by a layer of growing cells within the capsule, the octopus lens is composed of anterior and posterior joined parts, formed by layers of lentigenic cell processes extending from the external collar. Both trout and octopus have a strong refractive index gradient of similar form, increasing from the lens cortex to the centre over nearly the same index range (Fig. 3b). Similar gradients occur in a variety of fish (Mattheissen, 1882; Axelrod, Lerner & Sands, 1988; Jagger & Sands, 1996). This index gradient causes rays to follow nearly circular paths within the lens, adding power and correcting aberrations to form a bright sharp image. The advantage in image-forming ability over a spherical lens of homogeneous refractive index is very great

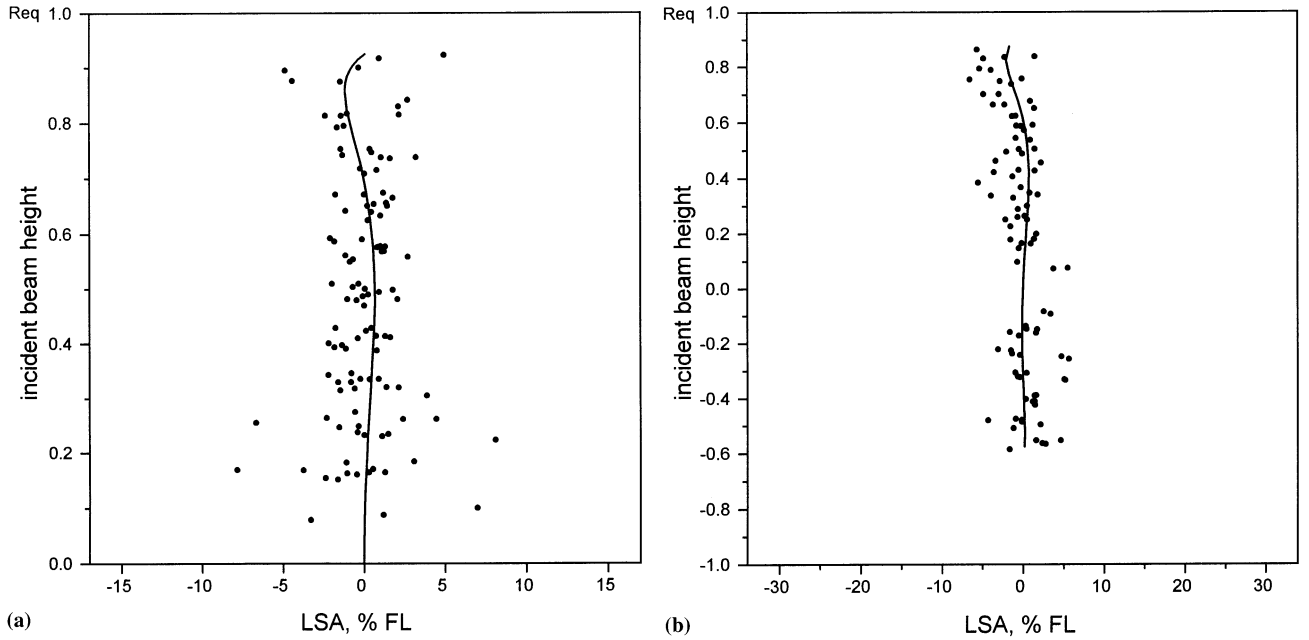

Fig. 6. Measured longitudinal spherical aberration on (a) and off axis at 45° (b) of five octopus lenses (points), and the calculated longitudinal spherical aberration of the model octopus lens (curves). The model curves describe the good correction for this aberration in the octopus lens.

(Jagger, 1992). The isoindicial curves measured in fish are more regular and circular than those measured for the octopus. Those in the octopus often show more deviation from circularity and a steeper gradient in the anterior portion, and the measured gradients in the equatorial direction (Fig. 3b) show some sigmoid structure. These variations may be in part measurement artefact. Gradient forms used for the lens models of octopus and fish are very similar (Fig. 3b). The small difference between them may result from the small differences in model lens shapes and cortical and core indices in these animals. The overall optical effect of the gradient in the octopus and trout is relatively good monochromatic aberration correction (Figs. 4–6, 8 and 11).

4.3. A wide, bright visual field and the influence of symmetry and pupil shape

In octopus and trout, spherical symmetry allows maintenance of a relatively bright and well-corrected retinal image far into the peripheral field, where retinal irradiance eventually declines because of obstruction by the eye cup (Fig. 10). The octopus pupil is nearly round under low light conditions and closes to a thin horizontal slit in strong light (Muntz, 1977). A horizontal slit-shaped pupil allows retinal irradiance to be maintained over a wide horizontal field. Foreshortening of the slit pupil aperture causes a more rapid decrease in retinal irradiance with vertical field angle, effectively shading light from above. The large round trout pupil is immobile, as in most teleosts, and does not offer control of retinal irradiance. Image irradiance of an extended object is proportional to the square of the relative aperture ($f/1.5$ for the full aperture octopus lens and $f/1.2$ for the trout), so that maximum retinal irradiance in the octopus is about 2/3 that of the trout.

Mattheissen's ratio, the focal length divided by the lens radius, has been used to compare aquatic eyes. For the nearly spherical octopus and trout lenses, it can be approximated by the focal length divided by the average of axial and equatorial radii. It is not as suitable for comparing light-gathering power as is relative aperture, because it is based on lens size rather than maximum pupil aperture. A low Mattheissen's ratio generally indicates high light-gathering ability, and different fish species show values of 2.2–2.8 (Mattheissen, 1882; Sroczyński, 1977). The value for trout of 2.38 lies about midway within this range, while the Mattheissen ratio for octopus, 2.83, lies at the upper limit of this range.

4.4. Accommodation by lens movement

Both octopus and fish accommodate by moving the entire lens. The lens in these animals is relatively rigid, an apparent correlate of high-index material, and accommodation by lens shape change as in higher animals does not occur. In many fish, lens movement occurs along an axis at a large angle to the eye's axis, allowing accommodation in the anterior binocular field (Somiya & Tomura, 1973). In the octopus, accommodation probably occurs by anterior globe shape changes that shift the lens primarily along the eye's axis (Beer, 1897; Hess, 1909). Accommodation in this direction is

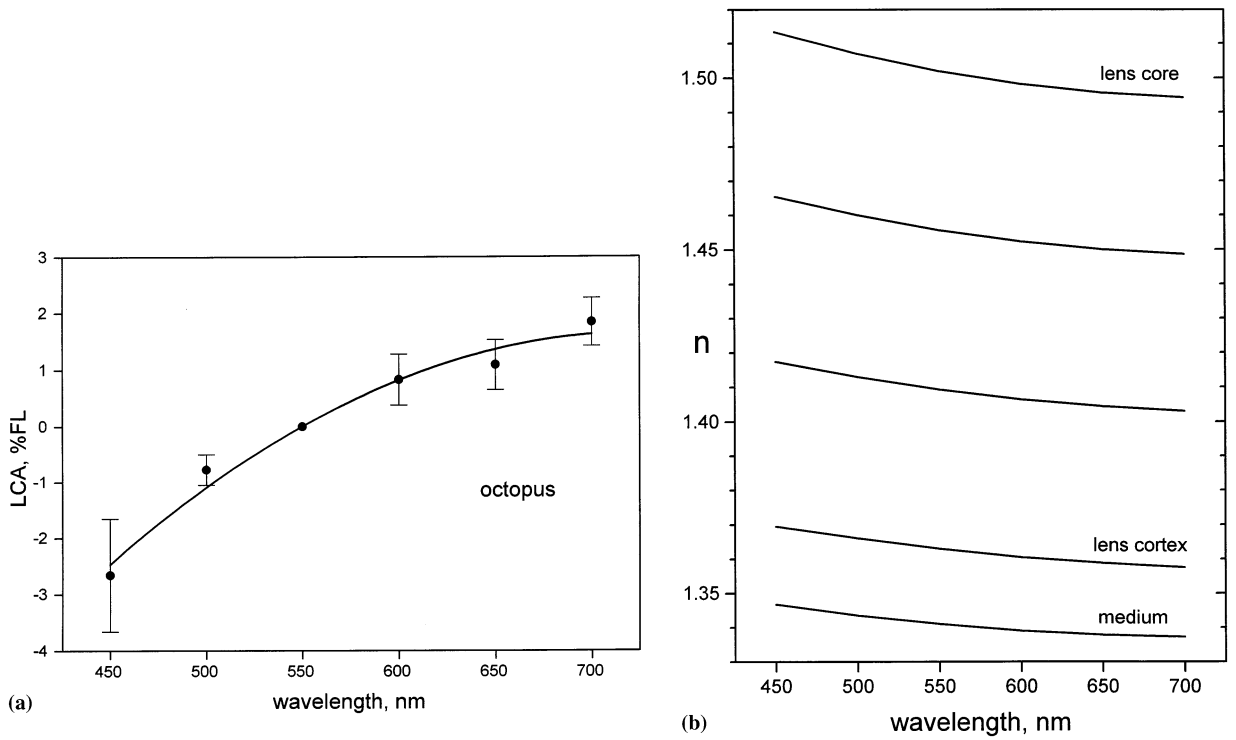

Fig. 7. (a) Chromatic axial focal shift as a function of wavelength (abscissa) caused by lens material dispersion shown in (b). At the retina, this focal shift degrades a white point object into a series of superimposed unfocussed coloured discs. Shown is measured chromatic axial focal shift (•) for five octopus lenses, with error bars of length twice the S.D. The solid curve is a best fit second degree polynomial, which coincides with the calculated model chromatic focal shift using the dispersion curves of (b).

appropriate in the octopus, because fixation is usually monocular. The focal surface of the octopus lens (Fig. 8) conforms to the retinal curvature (Fig. 1b). Superimposed on this figure are three model focal surfaces for objects at infinity (closest to lens), and 100 and 50 mm distant, and accommodative lens movements needed to place an image surface on the retina can be judged from their spacing.

4.5. Chromatic aberration of the lens and how it limits image quality

Longitudinal chromatic aberration will limit image quality in these lenses because only one wavelength can be in focus at a time. An image formed in sunlight therefore consists of unfocussed coloured images superimposed upon the focused image. Observed octopus lens longitudinal chromatic aberration or focal shift (Fig. 7a) is almost identical to that observed in trout, and lens model dispersion (Fig. 7b), similar in both animals, predicts this focal shift.

The limit imposed on the trout MTF by chromatic aberration can be calculated (Jagger, 1997). Detected image degradation will increase with object spectral bandwidth, receptor spectral bandwidth, chromatic aberration, and relative aperture. Given similar photic environments near the surface (trout and octopus frequent shallow water), and their similar rhodopsin-based retinal pigments, image quality in both species at full pupil aperture will be limited to a similar degree. The octopus retina has only one pigment, of λ_{max} 475 nm (Messenger, 1981), and the animal cannot discriminate colour. The adult trout has three cone pigments of λ_{max} 434, 531 and 576 nm (Hawryshyn & Hárosi, 1994), which allow it to discriminate colours. The chromatic limitation to the MTF will be similar for trout or octopus with lens size above about 1 mm diameter. For lenses much smaller, diffraction increasingly limits resolution.

4.6. Behaviour of the octopus lens model

The octopus lens model, constructed using parameter values based upon measurements, displays focal length and longitudinal spherical aberration close to the average values measured for the octopus lens. With material dispersion similar to that of other species, this model also predicts the measured chromatic aberration. Muntz and Gwyther (1988) measured octopus acuity of 3–7 c/deg. The calculated model MTF (an upper estimate) is consistent with this result, if the conservative assumption is made that the animal can discriminate contrast of 0.4 or less. Measured acuity lies well below the diffraction-limited MTF, which reaches zero at about 150 c/deg for a 5 mm pupil diameter.

The ability of this model to predict measured optical behavior indicates its suitability as a representation of the real lens. Its similarity to the trout lens model will extend to results described for the trout lens by Jagger and Sands (1996). These include the sensitivity of lens correction and focal length to variation of core and cortical indices, relative magnitudes of surface and internal powers, the interpretation of Schlieren image detail as gradient structure, and the course of rays through the lens.

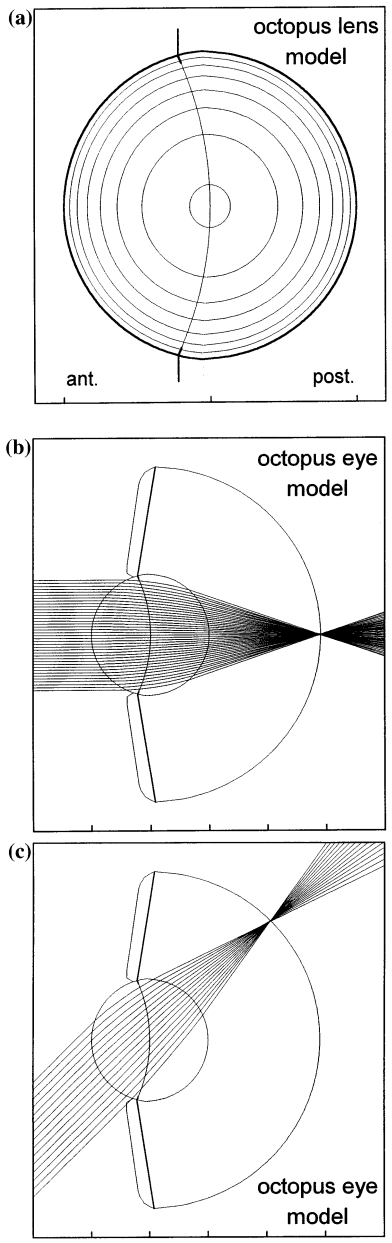

Fig. 8. (a) Axial section of the model octopus lens, showing external shape, boundary between anterior and posterior parts, suspending collar (heavy line) and internal isoindicial curves. Isoindicial curve interval is 0.02, from 1.38 (near the surface) to 1.50 (near the centre). (b) Diagram of a meridional fan of rays parallel to the axis and (c) at 45° to the axis refracted by the model octopus lens and eye, demonstrating the good optical correction of the model. Ticks on the lower border are spaced one model unit, equal to half the lens axial length.

4.7. Octopus lens secondary structure and image fine detail

Secondary fine structure observed in the trout lens can be identified as the source of certain features of image fine detail. In the octopus, light scattering within the lens is expected to cause speckle in the image, as in the trout. It could be incorporated in the model lens as a structural perturbation, as suggested for the trout model lens. The nearly smooth octopus Schlieren images (Fig. 5) contrast with the abrupt zonal discontinuities in those of the trout, and indicate better index continuity between adjacent layers in the octopus lens. Concentric structure in the point image as observed in the trout (Jagger, 1996) is therefore not expected. Radial structure, seen in the trout lens Schlieren image, is also not apparent in the octopus Schlieren image, and sharp radial spikes in the point image are also not expected in octopus. Secondary structures present in octopus but not in trout lens are the filamentous structures of about 30 μm thickness over the entire aperture. These may be lentigenic cell process boundaries. Their orientation seems random, and they will probably contribute to scattering.

4.8. Convergent evolution of eye design in octopus and trout

The remarkable similarity in eye optical design and function found in octopus and trout (Fig. 11) is the result of convergent evolution to a solution satisfying the needs of a predatory aquatic lifestyle. As we have shown, lenses of these two species are nearly functionally interchangeable. Darwin (1872) noted that beyond the superficial resemblance between the eyes of cuttlefish and vertebrates, there was hardly any real similarity. Our results show that although many details differ, the superficial resemblance between the eyes of octopus and trout originates from their similarity in basic optical design. Two common requirements that have channelled these designs along converging paths can be inferred:

4.8.1. The lens must provide all the eye's power

In the absence of an effective cornea, a spherical aquatic lens with a spherically symmetric internal index gradient offers considerable advantage. Over a wide field, such a lens offers high surface power, high gradient power from ray curvature within the lens, and relatively uniform image quality and retinal irradiance. High gradient power further requires a large difference between lens core and cortical indices, probably limited

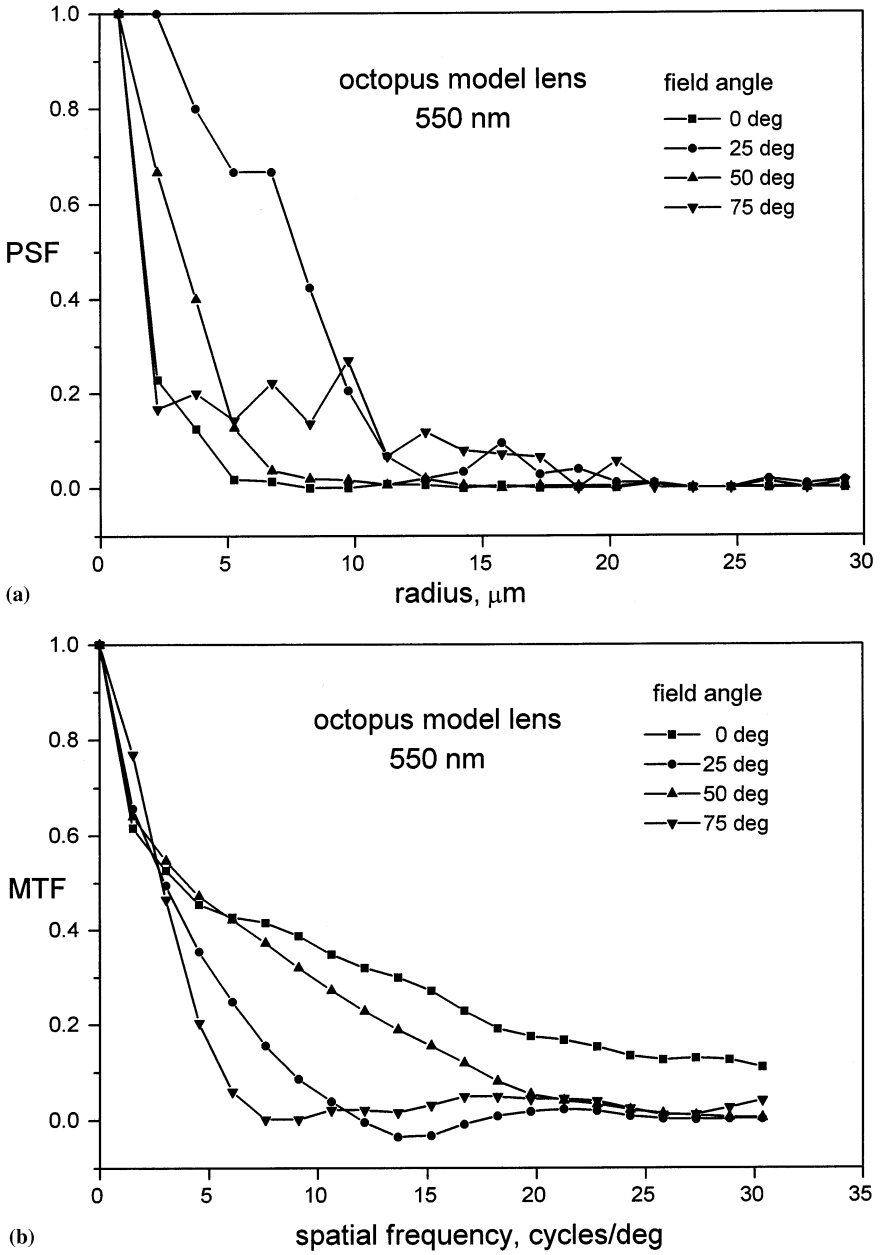

Fig. 9. (a) Calculated octopus model lens monochromatic pointspread functions (PSF) assuming axial thickness 6 mm and (b) modulation transfer functions (MTF) for various field angles for the full aperture octopus model lens. The MTF is independent of model scale. The optical resolution of the model octopus eye is well below the diffraction limit, about 170 c/deg for this lens.

by the upper and lower crystallin concentrations attainable.

4.8.2. A bright image is required in a compact eye

A bright image allows short integration time and rapid information transfer, useful in pursuit and evasion. It results from the large aperture and relatively short focal length of the lens (and hence compact eye) made possible by an internal index gradient that adds power and corrects aberration. Mattheissen's ratio (2.83 for octopus; 2.38 for trout) and the relative aperture (f/1.5 for octopus, f/1.2 for trout) indicate that the octopus eye has somewhat less light-gathering power than the trout eye, although within the reported range for fish (2.2–2.8). The 19% higher Mattheissen's ratio in octopus compared to trout results from its 16% lower gradient strength as measured by core-cortex index difference. It is not clear whether this represents a significant structural limit in the octopus, or whether it confers a functional advantage.

Strong longitudinal chromatic aberration limits the MTF and hence resolution in octopus and trout eyes (Jagger, 1997). As in other animal eyes, chromatic aberration is not corrected. Chromatic correction in

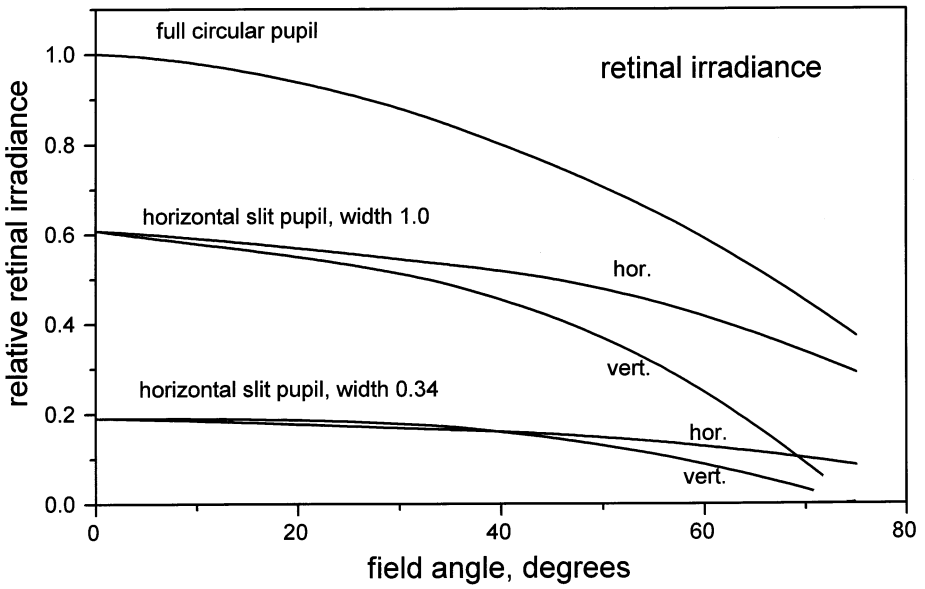

Fig. 10. Calculated relative retinal irradiance for full circular pupil and two horizontal slit pupil widths as a function of field angle (measured from the optical axis) for the model octopus eye. Retinal irradiance falls off with angle in the horizontal field because of unavoidable obstruction by the eye cup. In the vertical field, foreshortening of the slit pupil causes a more rapid decrease with angle.

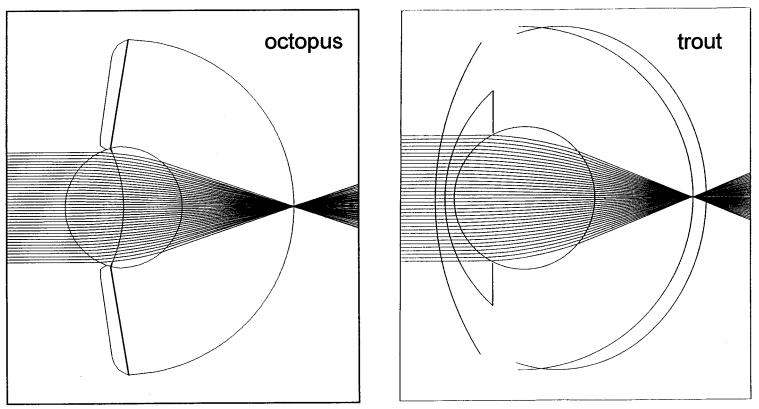

Fig. 11. The course of rays refracted by the model octopus eye compared with a model trout eye of the same diameter from Jagger and Sands (1996). Both eyes use a similar strong gradient of refractive index in a nearly spherical lens to form a bright image of good quality over a wide field. In the trout, immersion renders the cornea optically ineffective and the relative aperture is somewhat greater than in the octopus. Neither eye is corrected for longitudinal chromatic aberration.

manufactured optics requires materials of differing dispersive properties, a solution probably unavailable to the eye. Both animals apparently tolerate lowered resolution as a trade-off for a bright image. Better resolution might be obtained by lowering the relative aperture by means of a smaller effective pupil or receptor apertures or by operating in a photic environment of bandwidth narrower than that of sunlight.

Acknowledgements

Australian Research Council Grant A09330801 supported this work. The authors thank W.R.A. Muntz and A. Hughes for helpful discussions.

References

Amoore, J. E., Rodgers, K., & Young, J. Z. (1959). Sodium and potassium in the endolymph and perilymph of the statocyst and in the eye of *Octopus*. *Journal of Experimental Biology*, *36*, 709–714.

Arnold, J. M. (1967)). Fine structure of the development of the cephalopod lens. *Journal of Ultrastructure Research*, *17*, 527–543.

Axelrod, D., Lerner, D., & Sands, P. J. (1988). Refractive index within the lens of a goldfish eye determined from the paths of thin laser beams. *Vision Research*, *28*, 57–65.

Beer, T. (1897). Die Accommodation des Kephalopodenauges. *Pflügers Archiv*, *67*, 541–586.

Darwin, C. (1872). *The origin of species* (6th edn.). London: Murray.

Hawryshyn, C. W., & Hárosi, F. I. (1994). Spectral characteristics of visual pigments in rainbow trout (*Onchorhychus mykiss*). *Vision Research*, *34*, 1385–1392.

Heidermanns, C. (1928)). Messende Untersuchungen über das Formsehen der Cephalopoden und ihre optische Orientierung im Raume. *Zoologische Jahrbücher* (*allgemeine Zoologie und Physiologie*), *45*, 609–650.

Hess, C. (1909). Die Accommodation der Cephalopoden. *Archiv für Augenheilkunde*, *64*, 125–152.

Houstoun, R. A. (1930). *A treatise on light*. London: Longmans, Green.

Jagger, W. S. (1992). The optics of the spherical fish lens. *Vision Research*, *32*, 1271–1284.

Jagger, W. S., & Muntz, W. R. A. (1993). Aquatic vision and the modulation transfer properties of unlighted and diffusely lighted natural waters. *Vision Research*, *33*, 1755–1763.

Jagger, W. S., & Sands, P. J. (1996). A wide-angle gradient index optical model of the crystalline lens and eye of the rainbow trout. *Vision Research*, *36*, 2623–2639.

Jagger, W. S. (1996). Image formation by the crystalline lens and eye of the rainbow trout. *Vision Research*, *36*, 2641–2655.

Jagger, W. S. (1997). Chromatic and monochromatic optical resolution in the rainbow trout. *Vision Research*, *37*, 1249–1254.

Mattheissen, L. (1882). Ueber die Beziehungen, welche zwischen dem Brechungsindex des Kerncentrums der Krystalllinse und den Dimensionen des Auges bestehen. *Pflügers Archiv*, *27*, 510–523.

Messenger, J. B. (1981). Comparative physiology of vision in molluscs. In H. Autrum, *Handbook of sensory physiology*, vol. VII/6C (pp. 93–200). Berlin: Springer.

Moody, M. F., & Parriss, J. R. (1960). Discrimination of polarized light by *Octopus*. *Nature*, *186*, 839–840.

Muntz, W. R. A. (1977). Pupillary response of cephalopods. *Symposium of the Zoological Society of London*, *38*, 277–285.

Muntz, W. R. A., & Gwyther, J. (1988)). Visual acuity in *Octopus pallidus* and *Octopus australis*. *Journal of Experimental Biology*, *134*, 119–129.

Muntz, W. R. A., & Gwyther, J. (1989)). The visual acuity of octopuses for gratings of different orientations. *Journal of Experimental Biology*, *142*, 461–464.

Sands, P. J. (1984). Drishti, a computer program for analysing symmetrical optical systems incorporating inhomogeneous media. *Technical Report 8*. Canberra: CSIRO Division of Computing Research.

Somiya, H., & Tomura, T. (1973). Studies on the visual accommodation in fishes. *Japanese Journal of Ichthyology*, *20*, 193–206.

Sroczyński, S. (1977). Spherical aberration of crystalline lens in the roach, *Rutilus rutilus L. Journal of Comparative Physiology*, *121*, 135–144.

Sroczyński, S, & Muntz, W. R. A. (1985)). Image structure in *Eledone cirrhosa*, an octopus. *Zoologische Jahrbücher* (*Physiologie*), *89*, 157–168.

Sroczyński, S, & Muntz, W. R. A. (1987). The optics of oblique beams in the eye of *Eledone cirrhosa*, an octopus. *Zoologische Jahrbücher* (*Physiologie*), *91*, 419–446.

Packard, A. (1969). Visual acuity and eye growth in *Octopus vulgaris*. *Monitore Zoologico Italiano* (*N.S.*), *3*, 19–32.

Packard, A. (1972). Cephalopods and fish: the limits of convergence. *Biological Review*, *47*, 241–307.

Sivak, J. G. (1991). Shape and focal properties of the cephalopod ocular lens. *Canadian Journal of Zoology*, *69*, 2501–2506.

Vine, A. C. (1972). Oceanographic data. In D. E. Gray, *American institute of physics handbook* (pp. 2/119–2/132)). New York: McGraw-Hill.

Wentworth, S. L., & Muntz, W. R. A. (1992)). Development of the eye and optic lobe of Octopus. *Journal of Zoology*, *London*, *227*, 673–684.

West, J. A., Sivak, J. G., Pasternak, J., & Piatigorsky, J. (1994)). Immunolocalization of S-crystallins in the developing squid (*Loligo opalescens*) lens. *Developmental Dynamics*, *199*, 85–92.

Young, J. Z. (1971)). *The anatomy of the nervous system of Octopus vulgaris*. Oxford: Clarendon.